Detecting Temporal Correlation on HfO_2 Based RRAM on 65nm CMOS Technology

Sarah Rafiq
College of Nanoscale Science and Engineering
SUNY Polytechnic Institute
Albany, USA
rafiqs@sunypoly.edu

Minhaz Abedin
College of Nanoscale Science and Engineering
SUNY Polytechnic Institute
Albany, USA
abedinm@sunypoly.edu

Karsten Beckmann
College of Nanoscale Science and Engineering
SUNY Polytechnic Institute
Albany, USA
kbeckmann@sunypoly.edu

Nathaniel C. Cady
College of Nanoscale Science and Engineering
SUNY Polytechnic Institute
Albany, USA
cadyn@sunypoly.edu

***Abstract*—Hafnium-oxide based bipolar RRAM was investigated for high-level temporal correlation detection, for in-memory computing. The experimental analog data of HfO_2 RRAM, both in RESET and SET regimes was evaluated to detect 10 correlated processes from 25 processes on a 5x5 RRAM array. Our method gave 36,000-53,000 times less energy consumption than that of a previous implementation with phase change memory, and a predicted acceleration of 1600-2100 times the execution time than that of 1xPOWER8 CPU (1 thread) for detecting correlation between 25 processes.**

Keywords—RRAM, analog switching, in-memory computing, temporal correlation detection.

I. Introduction

The challenges faced in complementary metal-oxide semiconductor (CMOS) scaling, due to the decline of Moore's law and end of Dennard's scaling, has inspired the search for alternatives to the standard von Neumann architecture [1-3]. The rapid increase of ever-growing number of devices with the advent of Internet of Things (IoT), gives rise to an explosion of data that need to be processed. The bottleneck between memory and processor therefore incurs significant power consumption and latency, in addition to limited bandwidth. The data transfer of operands between memory and processor consumes a few hundred times more energy than the computation itself [2]. An alternative would be to collocate memory and processor, to process data where it is stored. Thus emerging non-volatile memory technologies are attractive for such applications.

Resistive random access memory (RRAM), among other non-volatile memories, is good candidate due to its high switching speed, high density, good CMOS compatibility, simple structure and ease of fabrication [4]. It is a two-terminal device whose resistance can be modulated through applied electrical pulses. As such, they have been used to accelerate vector-matrix multiplications [5-6], and realize classification tasks in neuromorphic computing. Array structures of RRAM is common, and can be used for in-memory computations In addition, logic operations in-memory such as IMPLY and FALSE, MAGIC, and flow-based computing have been proposed on memory arrays [7-10]. Correlation shows the degree of association between two variables [11]. Correlation detection may be applicable for IoT, social networks, large scientific data, where data may be processed into binary data streams [12]. The correlation between these binary data streams may be carried out in real-time to identify clusters of correlated data in incoming data streams [12]. Correlation was previously detected using phase change memory (PCM), where the crystallization dynamics of PCM was used to determine correlated statistical event-based data streams [12] and in another example, a single-neuron computational primitive and a level-tuning concept [13]. RRAM has different operating principles than PCM, and consumes lower RESET programming power, has simple fabrication requirements, is CMOS compatible, and has high switching speeds. Thus, RRAM warrants investigation for this application; however, this high level computation has been simulated with RRAM model [14], but has not been investigated with actual RRAM analog performance characteristics. In this work the analog switching data of actual RRAM devices were investigated with a temporal correlation detection algorithm.

II. RRAM Fabrication and Characterization

A. RRAM Fabrication

The hafnium oxide based RRAM used in this work consists of TiN/Ti/HfO_2/TiN stack, where the top and bottom electrodes are TiN, HfO_2 is the switching layer and the Ti is oxygen exchange layer (OEL). The RRAM was integrated with 65nm CMOS technology on a 300mm wafer platform. The RRAM was implemented between M1/V1 interface, to form 1-transistor-1-RRAM structures.

B. Electrical Charactrerization of Analog Switching of RRAM

A high frequency electrical measurement setup consisting of Berkeley Nucleonics pulse generator, power splitter, and radio frequency (RF) probes, was used to generate and apply the ultra-short pulses to 1T1R devices. The pulse generator input was fed into a power splitter, which split 50% of the input and applied to the top electrode of 1T1R, and the other 50% was connected to oscilloscope to display the applied pulse train. A 50 Ohm termination resistance between the probes and the power splitter is used to minimize signal reflection. Due to ultra-short pulse widths down to 300ps this measurement setup required extra

pads to accommodate 1T1R device testing. Thus, this imposed a limitation to apply ultra-short pulses to an array of connected

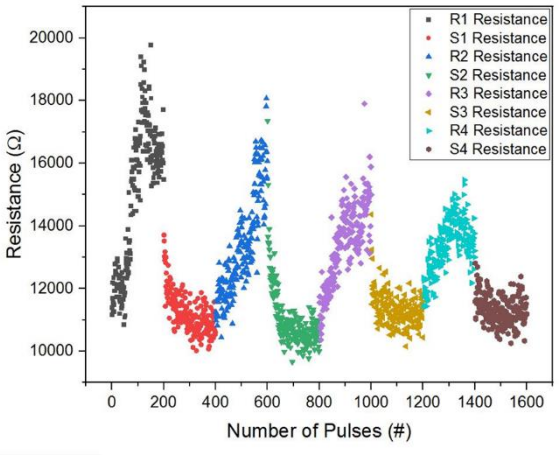

Fig. 1. Analog switching data using ultra-short 300ps pulses of 200 RESET pulses followed by 200 SET pulses, for four cycles. The four cycles for RESET and SET were denoted by R1-R4 and S1-S4, respectively, using different colors. The SET and RESET voltages used are 1V and -0.75V, respectively, of 300ps duration. After each SET/RESET pulse, a read-verify approach was used to measure the intermediate resistance states.

1T1R devices. Therefore, the measurement results were used in the simulation of temporal correlation detection in a Python environment.

After forming the RRAM devices at 3V, 200 RESET pulses followed by 200 SET pulses, of 300 picosecond pulse widths, were applied consecutively to gradually modulate the RRAM resistance from LRS to HRS (RESET) and HRS back to LRS (SET). The SET and RESET voltages were fixed at 1V and -0.75V, respectively. The positive voltage was applied in succession to decrease RRAM resistance gradually while the negative voltage was applied in succession to increase RRAM resistance gradually, as shown in Fig. 1. Higher RESET voltage amplitudes resulted in higher variability along with higher resistance for HRS [15]. Therefore, to reduce resistance variability a lower RESET voltage amplitude was used. After each SET or RESET pulse, a read pulse of -0.3V of 10 µs duration was applied to read the intermediate resistance. Multiple devices were measured. The data for four cycles are shown in Fig. 1. The application of ultra-short pulses gives the monotonic change in device resistance and the accumulative behavior that is employed in the temporal correlation detection algorithm. The data in the respective four SET and RESET cycles in Fig. 1 are denoted by S1-S4 cycles and R1-R4 cycles, respectively. These cycles were used to detect temporal correlation between binary processes, and the effect of data in each cycle on the temporal correlation detection algorithm is discussed.

III. Temporal Correlation Detection using RRAM

A. Generation of Correlated and Uncorrelated Processes

The discrete-time binary stochastic processes, X_i, are first generated and then assigned to a 5x5 array. The correlated processes were generated with a binomial distribution with P(X=1)=0.1, over a large time instant, and are correlated with a correlation coefficient of 0.8. The correlation coefficient, c, between two binary processes, $X_i(k)$ and $X_j(k)$, is given in equation (1) [11-12,14]. This normalizes the covariance between the two random variables, and varies from -1 to 1. If the two processes are correlated, the c>0. Otherwise, the processes are not correlated.

$$c = \frac{Cov[X_i(k), X_j(k)]}{\sqrt{Var[X_i(k)] * Var[X_j(k)]}} \quad (1)$$

The ten correlated processes were assigned to the first two rows of the 5x5 array. The rest of the array were assigned uncorrelated processes.

B. Algorithms for Temporal Correlation Detection using SET and RESET Regimes

The temporal correlation detection algorithm was adapted from [12], but the algorithm was modified to work with the RRAM analog data, both in RESET and SET regimes, of fixed pulse amplitude and pulse width. The experimental RRAM data is used to update RRAM resistance in simulation.

As each binary process, X_{ij}, was assigned to each RRAM device in the 5x5 array, the row and column of RRAM and its assigned process are denoted by i and j, respectively. The value of binary process, Xij(k), is either 0 or 1 at time instant k. The algorithm of temporal correlation detection with RESET data and SET data are shown in Figures 1 and 2 respectively. Firstly, the entire array is SET (RESET) to high (low) conductance if the RESET (SET) regime of RRAM is used in simulation at k=0. This conductance is taken from the last datum of previous SET (RESET) cycle. The parameters time instant k, momentum M and the number of pulses applied n, are initialized. Then, an instantaneous sum of all processes is calculated in the first loop, called M(k), at each time instant k. Then, the M(k) determines the number of programming pulses to be applied to RRAM device if its assigned process Xij(k) holds a non-zero value. The M(k) modulates the number of applied pulses instead of pulse amplitude, based on the function f(M), shown in Equation 2. This eliminates the need of a constant required in previous algorithm to keep within switching thresholds.

$$f(M) = \begin{cases} 1 & 1 \le M(k) < 3 \\ 2 & 3 \le M(k) < 10 \\ 3 & 10 \le M(k) < 15 \\ 4 & 15 \le M(k) < 20 \\ 5 & 20 \le M(k) < 25 \\ 0 & Otherwise \end{cases} \quad (2)$$

The parameter n ensures that only 200 pulses are applied during resistance modulation, and that the RRAM resistance saturates at the 200th applied pulse and maintains this resistance for subsequent pulses. After the number of pulses to be applied, y, based on f(M), is determined, the RRAM Rij where Xij(k)=1 is applied y number of RESET pulses in Figure 1 and y number of SET pulses in Figure 2. The parameter pulse_no ensures that y number of pulses are applied to the RRAM device Rij. As each RESET (SET) pulse is applied, the resistance of Rij is updated from the RESET (SET) cycle analog data, R1-R4 (S1-S4). This is checked for all the 25 processes, then the time instant k is incremented and the M(k) is reset to 0. This algorithm iterates

Research sponsored by National Science Foundation, under award number 1823015.

until the final time instant k_{final}. The devices with correlated processes are expected to have greater absolute change in conductance than devices with uncorrelated processes. To compare whether the algorithm worked or not with the RESET

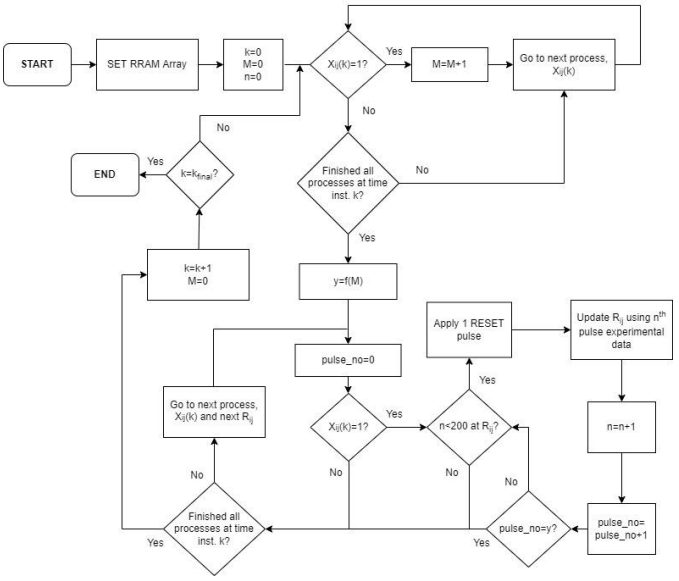

Fig. 2. Algorithm of the simulated temporal correlation detection with reset cycles R1-R4 of the RRAM analog switching data using 200 RESET pulses of 300ps pulse width.

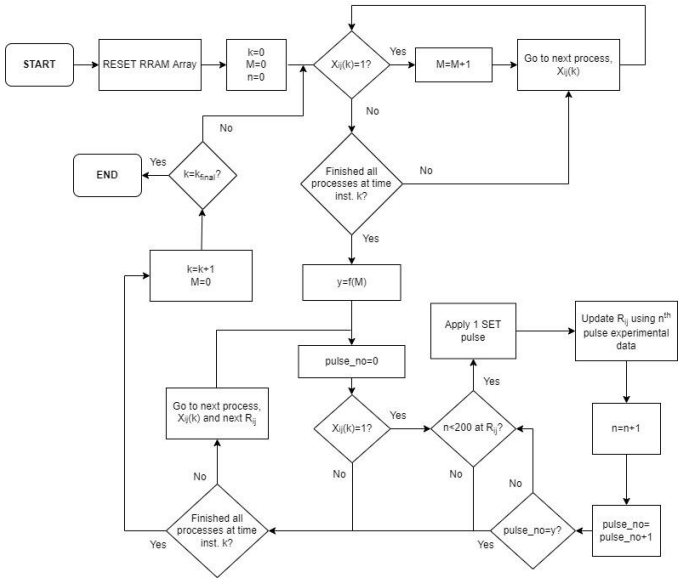

Fig. 3. Algorithm of the simulated temporal correlation detection with set cycles S1-S4 of the RRAM analog switching data using 200 SET pulses of 300ps pulse width.

and SET analog data, the difference between median conductance of devices with all correlated and uncorrelated processes are determined. The same processes were used for the RESET analog data in R1-R4 cycles and SET analog data in S1-S4 cycles. Lastly, the devices with correlated processes are expected to have greater change to low conductance (high conductance) when RESET (SET) data is used.

IV. Results and Discussion

The temporal correlation detection results with analog RESET cycles, R1-R4, are shown for time instants k of 500, 600, 900, 1200 and 1300 in Figures 4-8, respectively. The temporal correlation detection results with analog SET cycles, S1-S4, are shown for time instants k of 130, 317 and 1200 in Figures 9-11 respectively. The algorithm uses the non-volatile accumulative behavior of RRAM shown in Figure 1.

A. Results of R1 RESET Cycle Analog Data

In the analog RESET R1 cycle, resistance increases gradually from 11 kΩ to 19 kΩ in the initial 130 pulses and hits a peak, then decreases till 200th pulse. This resulted in greater

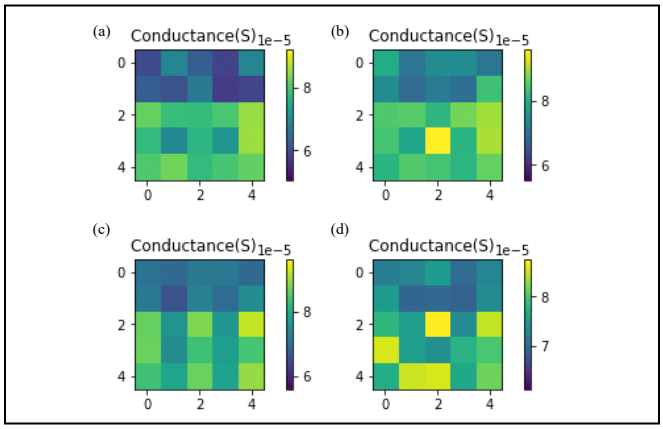

Fig. 4. Conductance of 5x5 RRAM array at time instant k=500 using analog a) R1 reset cycle data b) R2 reset cycle data c) R3 reset cycle data and d) R4 reset cycle data.

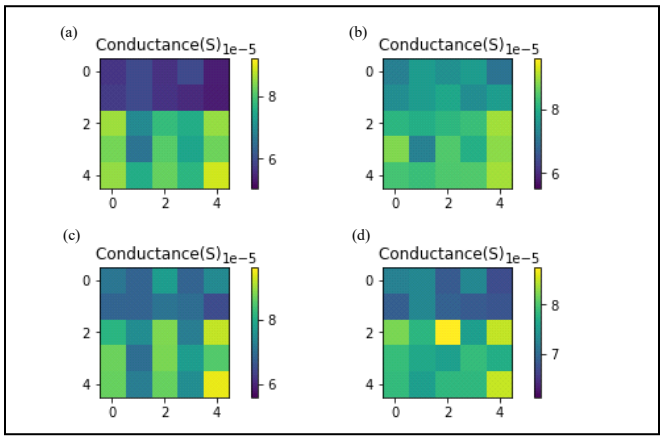

Fig. 5. Conductance of 5x5 RRAM array at time instant k=600 using analog a) R1 reset cycle data b) R2 reset cycle data c) R3 reset cycle data and d) R4 reset cycle data.

absolute change in conductance for devices with correlated processes with the initial 130 pulses, and detected the correlated processes at time instants k=500, 600 in Figures 4(a) and 5(a) respectively. However, due resistance decrease after 130 pulses, the algorithm fails to detect the correlated processes when it iterates to higher time instants k of 900, 1200 and 1300 in Figures 6(a), 7(a) and 8(a), respectively. This shows that gradual monotonic resistance modulation is important for the

algorithm to work. The difference in median conductance of correlated and uncorrelated processes is 20 µS at k=500, 600 when all correlated processes were detected.

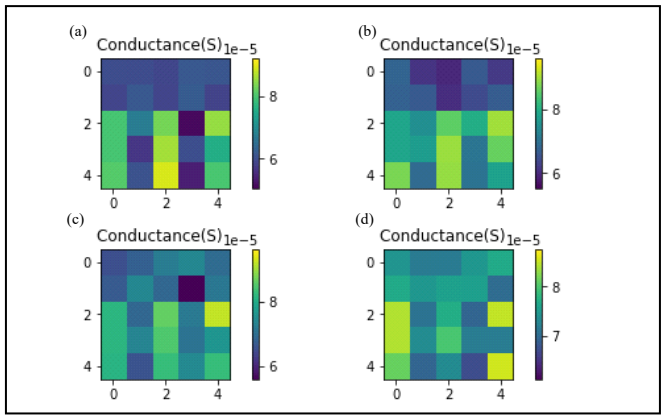

Fig. 6. Conductance of 5x5 RRAM array at time instant k=900 using analog a) R1 reset cycle data b) R2 reset cycle data c) R3 reset cycle data and d) R4 reset cycle data.

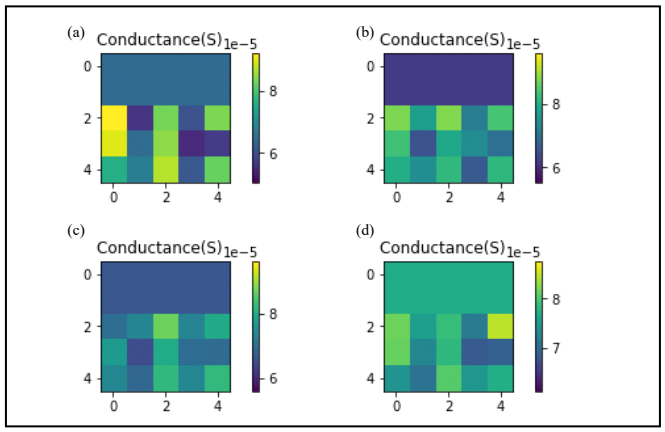

Fig. 7. Conductance of 5x5 RRAM array at time instant k=1200 using analog a) R1 reset cycle data b) R2 reset cycle data c) R3 reset cycle data and d) R4 reset cycle data.

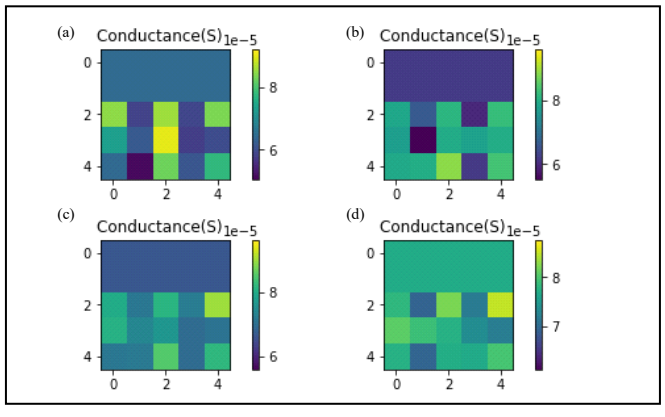

Fig. 8. Conductance of 5x5 RRAM array at time instant k=1300 using analog a) R1 reset cycle data b) R2 reset cycle data c) R3 reset cycle data and d) R4 reset cycle data.

B. Results of R2 RESET Cycle Analog Data

In the analog RESET R2 cycle, resistance increases gradually from 10.5 kΩ to around 17 kΩ with 200 successive RESET pulses, giving a monotonic resistance change despite the variability present. This resulted in greater absolute change in conductance for devices with correlated processes at time instants k of 900 and 1200 shown in Figures 6(b) and 7(b), respectively. Similar data trends like R2 RESET cycle data also worked well (78%) with the algorithm. For earlier time instants k of 500 and 600, the correlated processes were not detected as shown in Figures 4(b) and 5(b) respectively. This may be due to RRAM resistance variability present. For later time instant k of 1300, the algorithm could not detect the correlated processes because the devices already reached saturated conductance at 200th pulse as shown in Figure 8(b), and this final datum is not the lowest conductance present in the R2 RESET cycle data. For k of 500 and 600 where algorithm detected all correlated processes, the difference in median conductance of devices with correlated and uncorrelated processes is 15µS.

C. Results of R3 RESET Cycle Analog Data

In the analog RESET R3 cycle, resistance increases gradually from 10 kΩ to around 16 kΩ with 100 successive RESET pulses, then no resistance modulation with mean of 14 kΩ with standard deviation of 830 Ω for the next 100 successive RESET pulses. The temporal correlation detection detected the correlated processes with the first 100 pulses at time instant k of 500 shown in Figure 4(c). The algorithm then failed to detect the correlated processes in regions where there is no resistance modulation in the R3 RESET data, as shown in Figures 5(c), 6(c) and 7(c) for time instants 600, 900 and 1200, respectively. At the later time instant k of 1300, due to last datum in R3 RESET data being at lowest conductance, the correlated processes were detected when the conductance saturated as shown in Figure 8(c). These results show that the gradual resistance modulation in increasing resistance in the RESET is important for the algorithm to work. The absolute difference in median conductance between devices with correlated and uncorrelated processes where the correlated devices were detected at k of 500 and 1300, is 9.9µS.

D. Results of R4 RESET Cycle Analog Data

In the analog RESET R4 cycle, resistance increases gradually from 11.4 kΩ to 15 kΩ with the first 130 successive RESET pulses, then the resistance decreases till the 200th pulse. The algorithm detected all the correlated processes at time instant k of 600 using the initial 130 pulses of RESET R4 data, as shown in Figure 5(d). As expected, the resistance decrease after the 130 pulses resulted the algorithm to fail for time instants k of 900, 1200 and 1300 as shown in Figures 6(d), 7(d) and 8(d), respectively. The correlated processes were not detected at earlier time instant k of 500 as shown in Figure 4(d), and this may be due to resistance variation and the lower resistance range in initial RESET R4 cycle data. At k of 600, where there is greater absolute change of resistance in devices with correlated processes, the absolute median difference between the correlated and uncorrelated processes is 9µS. These results again show that the gradual resistance modulation in increasing resistance in the RESET is important for the algorithm to work.

E. Results of S1 SET Cycle Analog Data

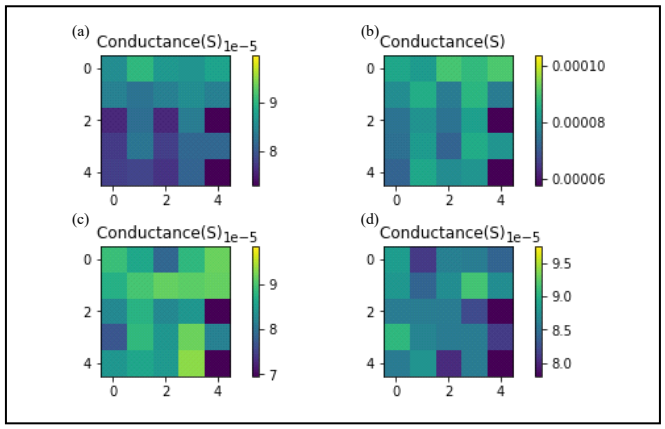

Fig. 9. Conductance of 5x5 RRAM array at time instant k=130 using analog a) S1 set cycle data b) S2 set cycle data c) S3 set cycle data and d) S4 set cycle data.

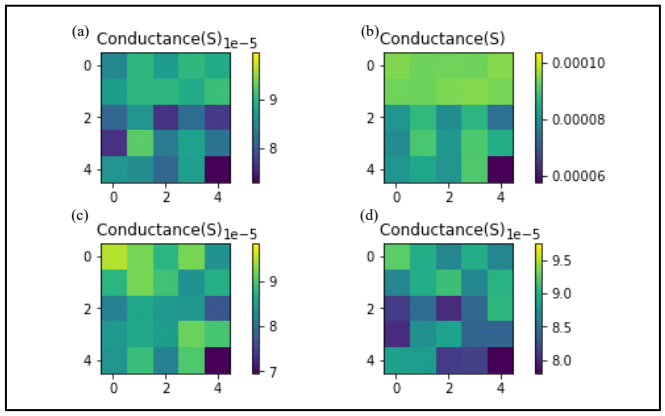

Fig. 10. Conductance of 5x5 RRAM array at time instant k=317 using analog a) S1 set cycle data b) S2 set cycle data c) S3 set cycle data and d) S4 set cycle data.

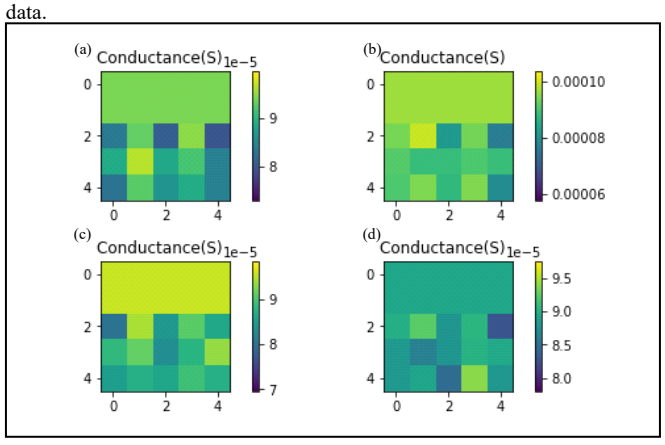

Fig. 11. Conductance of 5x5 RRAM array at time instant k=1200 using analog a) S1 set cycle data b) S2 set cycle data c) S3 set cycle data and d) S4 set cycle data.

In the analog SET S1 cycle, the resistance decreases gradually from 14 kΩ to 11.5 kΩ with the first 35 successive SET pulses, then no resistance modulation for next 55 successive SET pulses, followed by two dips in resistance with an average resistance of 11 kΩ with standard deviation of 410Ω till the 200th pulse, resulted in poor performance with the algorithm. At best, the algorithm only detected 90% of all correlated processes at time instant k of 130 using the initial 35 pulses, as shown in Figure 9(a). The algorithm failed to detect correlated processes at later time instants k of 317 and 1200 as shown in Figures 10(a) and 11(a) respectively. However, similar data trends for incremental SET pulses that decreases resistance monotonically with measurable resistance differences between initial and later cycles resulted in better performance with the algorithm. The absolute difference in median conductance of correlated and uncorrelated processes is 7 µS.

F. Results of S2 SET Cycle Analog Data

In the analog SET S2 cycle, the resistance decreases gradually from 14 kΩ to 10.5 kΩ with the first 70 successive SET pulses, then no resistance modulation due to resistance plateau at 10.5 ± 0.5 kΩ, as shown in green in Figure 1. Thus, using the initial 70 pulses, the temporal correlation detection algorithm detected 50% and 100% of the correlated processes at time instants k of 130 and 317, as shown in Figures 9(b) and 10(b), respectively. Due to no resistance modulation in subsequent pulses of S2 SET data, the correlated processes were not detected at later time instant k of 1300 as shown in Figure 11(b). The final datum is also at 10.3 kΩ, so it is close to average resistance of the plateau and hence did not give much resistance difference. For k of 317, where the temporal correlation detection detected all the processes, the absolute difference in median conductance of devices with correlated and uncorrelated processes is 12 µS.

G. Results of S3 SET Cycle Analog Data

In the analog SET S3 cycle, the resistance decreases gradually from 14 kΩ to 11.2 kΩ with the first 20 successive SET pulses, then the resistance plateaus at 11.2 ± 0.43 kΩ. The algorithm failed to detect the correlated processes at time instants k of 130 and 317, as shown in Figures 9(c) and 10(c), respectively. This is because of negligible resistance modulation in the plateau and resistance variation present in this regime. Meanwhile, the algorithm detected the correlated processes at later time instant k of 1200, as shown in Figure 11(c), due to the last datum of S3 SET data being at lower resistance of 10.4 kΩ than rest of the data in the plateau. Thus, it gave greater absolute change in conductance when the resistance saturated at the 200th SET pulse. Data trends similar to this trend worked 77% with the correlation detection algorithm. At k of 1200, the absolute difference in median conductance of devices with correlated and uncorrelated processes is 8.3 µS.

H. Results of S4 SET Cycle Analog Data

In the analog SET S4 cycle, the resistance decreases gradually from 12.3 kΩ to 10.4 kΩ with the first 100 successive SET pulses, then resistance starts increasing back to 11.9 kΩ for subsequent SET pulses. This resulted in poor performance with the algorithm, as the resistance increased to the some of the highest resistance points in the regime during the last 100 SET pulses, comparable to those at initial points in S4 SET data. This did not give much change in absolute conductance, and hence algorithm failed to detect all correlated processes at time instants

k of 130, 317, 1200 shown in Figures 9(d), 10(d) and 11(d), respectively. At best, the algorithm only detected 50% of the correlated processes during the first 50 pulses at time instance k of 255. At this time instant, the difference in median conductance of devices with correlated and uncorrelated processes is 3 μs.

I. Energy Consumption

The energy consumption of temporal correlation detection between 25 processes using analog switching of RRAM RESET and SET regimes are 27.7 pJ and 41 pJ, respectively. If correlation is detected at the same time instant k, for SET and RESET analog data, the energy consumption for SET analog data is higher than that of RESET, due to higher power consumption of each pulse due to higher pulse amplitude of 1V (versus -0.75V for RESET) and higher current because of lower programmed resistance. For temporal correlation detection using SET regime of PCM devices, the energy consumption for 25 processes is estimated to be 1.47 μJ [12]. Therefore, RRAM being used for temporal correlation detection leads to 36,000-53,000 less energy consumption than that of PCM. Also, due to the 300 ps pulse width, our method provides a speed-up of execution time by 1,600-2,100 times than that of 1xPOWER8 CPU [1 thread], for detecting temporal correlation between 25 processes [12].

V. Conclusion

A high-level computational primitive, temporal correlation detection, was performed using HfO_2 RRAM analog data as an in-memory computation. Four RESET and SET cycles, each consisting of 200 pulses, of fixed amplitude and pulse width, was assessed with modified temporal correlation detection algorithm. The abrupt SET and gradual RESET behavior of RRAM, due to different conduction mechanisms responsible for the SET and RESET operations, has an effect on the performance of the algorithm. The RESET cycles of analog data, R1, R2, R3, R4, show that the absolute difference in median conductance between the devices with correlated and uncorrelated processes were 20 μS, 15 μS, 9.9 μS and 9 μS, respectively, when 100% of correlated processes were detected. However, for SET cycles of analog data, S1, S2, S3, the absolute difference in median conductance between the devices with correlated and uncorrelated processes were 7 μS, 12 μS, 8.3 μS, respectively, when 100% of correlated processes were detected. For S4 SET cycle analog data, only 50% of the correlated processes were detected and resulted in absolute difference in median conductance between the devices with correlated and uncorrelated processes of 3 μS. The gradual resistance modulation, in a monotonic direction (either increasing or decreasing) is crucial for the algorithm to work. If there are regions of no resistance modulation, the algorithm fails to detect all the correlated processes. Lastly, the RESET regime seemed to work better with the algorithm due to the higher absolute change of conductance achieved for correlated processes, as evident by greater absolute difference in the median conductance of correlated and uncorrelated processes. An array of RRAM devices can thus be used to determine correlated processes from the uncorrelated binary processes, which can lead to improvements in energy consumption. Detecting temporal correlation between 25 processes using RRAM array gave 36,000-53,000 times less energy consumption than that of PCM array in [12], and a speed-up of 1,600-2,100 times the execution time than that of 1xPOWER8 CPU (1 thread) [12]. This demonstrates the low power consumption capability of RRAM for high-level computation.

VI. Acknowledgement

This research was sponsored by the National Science Foundation, under award number 1823015.

VII. Reference

[1] M. M. Waldrop. “The chips are down for Moore's law", *Nat.*, vol. 530, pp. 144-147, 2016.

[2] J. Shalf ,“The future of computing beyond Moore’s Law”, *Phil. Trans. R. Soc. A.*, vol. 378, no. 2166, Jan. 2020.

[3] T. Muttaqi, T. L. Baldwin and S. C. Chiu, "Distribution System State Estimation with AMI Based on Load Correction Method," *2019 North American Power Symposium (NAPS)*, 2019, pp. 1-6, doi: 10.1109/NAPS46351.2019.9000334.

[4] H. . -S. P. Wong et al., "Metal–Oxide RRAM," in *Proceedings of the IEEE*, vol. 100, no. 6, pp. 1951-1970, June 2012, doi: 10.1109/JPROC.2012.2190369.

[5] V. Milo, C. Zambelli, P. Olivo, et al. “Multilevel HfO2-based RRAM devices for low-power neuromorphic networks,” in *APL Mater*., vol. 7, no. 8, Aug. 2019, doi: 10.1063/1.5108650.

[6] M. Hu et al., "Dot-product engine for neuromorphic computing: Programming 1T1M crossbar to accelerate matrix-vector multiplication”, *Proc. 53rd Annu. Design Autom. Conf. (DAC)*, Austin, TX, USA, 2016, pp. 1-6, doi: 10.1145/2897937.2898010.

[7] J. Borghetti, G. S. Snider, P. J. Kuekes, J. J. Yang, D. R. Stewart, and R. S. Williams, “Memristive switches enable stateful logic operations via material implication,” *Nature*, vol. 464, no. 7290, pp. 873–876, 2010.

[8] S. Kvatinsky et al., "MAGIC—Memristor-Aided Logic," in *IEEE Transactions on Circuits and Systems II: Express Briefs*, vol. 61, no. 11, pp. 895-899, Nov. 2014, doi: 10.1109/TCSII.2014.2357292.

[9] J. S. Pannu et al., "Design and Fabrication of Flow-Based Edge Detection Memristor Crossbar Circuits1," *in IEEE Transactions on Circuits and Systems II: Express Briefs*, vol. 67, no. 5, pp. 961-965, May 2020, doi: 10.1109/TCSII.2020.2984155.

[10] S. Rafiq et al., "Investigation of ReRAM Variability on Flow-Based Edge Detection Computing Using HfO_2-Based ReRAM Arrays," in *IEEE Transactions on Circuits and Systems I: Regular Papers*, vol. 68, no. 7, pp. 2900-2910, July 2021, doi: 10.1109/TCSI.2021.3072210.

[11] A. G. Asuero and A. Sayago and A. G. González, “The Correlation Coefficient: An Overview,” in *Critical Reviews in Analytical Chemistry*, vol. 36, no. 1, 2006, doi:10.1080/10408340500526766.

[12] A. Sebastian, T. Tuma, N. Papandreou, M. Le Gallo, L. Kull, T. Parnell and E. Eleftheriou, “Temporal correlation detection using computational phase-change memory,” *Nat. Comm*., vol.8, no. 1115, 2017.

[13] A. Pantazi, S. Woźniak, T. Tuma and E. Eleftheriou, “All-memristive neuromorphic computing with level-tuned neurons”, *Nanotechnology*, vol. 27, no. 35, pp. 355205, Jul. 2016, doi: 10.1088/0957-4484/27/35/355205.

[14] S. Rafiq, K. Beckmann and N. C. Cady, "Simulation of Temporal Correlation Detection using HfO2-Based ReRAM Arrays," *2020 IEEE Student Conference on Research and Development (SCOReD)*, 2020, pp. 1-3, doi: 10.1109/SCOReD50371.2020.9250970.

[15] K. Beckmann, W. Olin-Ammentorp, G. Chakma, S. Amer, G. S. Rose, C. Hobbs, J. V. Nostrand, M. Rodgers, N. C. Cady, “Towards Synaptic Behavior of Nanoscale ReRAM Devices for Neuromorphic Computing Applications,” *ACM Journal on Emerging Technologies in Computing Systems*, vol. 16, no. 2, April 2020, doi: https://doi.org/10.1145/3381859.